RSC Advances

PAPER

View Article Online
View Journal | View Issue

Cite this: *RSC Adv.*, 2022, **12**, 24998

A simple synthesis of surfactant-free polycrystalline CuO nanoparticles supported on carbon nanofibers for regioselective hydroboration of alkynes†

Balaji Mohan,[abc] Kyung Hee Oh,[de] Ji Chan Park,*[d] Mohammad Yusuf,[c] Kang Hyun Park*[c] and Buhyun Youn*[a]

Received 26th July 2022
Accepted 23rd August 2022

DOI: 10.1039/d2ra04668g

rsc.li/rsc-advances

Copper oxide nanoparticles (CuO NPs) with a clean surface supported on carbon nanofibers (CNFs) in one-pot were prepared by simple solid-state grinding and aging followed by thermal treatment, yielding CuO nanoparticles with high (23.8 wt%) and uniform CuO loading in the absence of surfactants and solvent. The CuO NPs on CNFs (CuO/CNF) showed excellent catalytic activity in transforming a wide variety of alkynes into alkenyl boronates using B_2Pin_2 as a boron source in the absence of ligand and additives with high regioselectivity under mild conditions. Moreover, the present CuO/CNF catalyst was recyclable and possesses excellent chemoselectivity. The developed green synthetic approach is expected to offer exciting opportunities for designing monometallic or bimetallic nanoparticle catalysts on different supports applied in heterogeneous catalysis.

1. Introduction

Supported metal/metal oxide nanoparticles as solid heterogeneous catalysts have been widely used in many fields.[1] In particular, supported non-noble metals (*e.g.*, Co, Ni, Cu, *etc.*) have attracted great attention owing to their low costs and the ability to substitute noble-metal based catalysts in industrially important catalytic applications.[2] However, the catalytic efficiency of non-noble metal based catalysts is still inferior to that of noble-metal counterparts owing to low activity and poor generality.[3] To compensate the barrier, a high loading of non-noble metals with high dispersity needs to be supported. With a high level of nanoparticle loading, metal dispersion is very challenging due to the agglomeration of metal nanoparticles.[4] Therefore, high loading with high dispersity is a critical factor for non-noble metal catalysts.

In general, supported metal nanoparticle catalysts have been prepared *via* classical techniques such as impregnation and drying,[5] deposition–precipitation,[6] and ion-adsorption.[7] Other alternative processes like chemical vapor deposition, atomic layer deposition, surface functionalization, or combined procedures have also been used. However, impregnation and drying with metal nitrate salts as a precursor is the most common preparation and routine technique because of its convenience, easy solubility, and inexpensive starting materials that can readily decompose. However, the catalysts obtained are with inhomogeneous nanoparticle dispersion and distribution, because of weak support–precursor interactions.[8] Hence, high loading in the form of small nanoparticles still continues to be a challenge.

Herein, we present a simple solid-state grinding method as a strategy to anchor CuO nanoparticles with a high load (nominally 23.8 wt%, Cu base: 20 wt%). The technique, in which copper hydrate salts that melt before they decompose can be adsorbed to the surface of carbon nanofibers with no use of solvent.[9] The method is very simple and reproducible for the synthesis of the CuO/CNF.

Organoboron compounds are versatile building blocks in organic synthesis. In particular, *E*-alkenyl boronate esters are essential units to fabricate important drugs such as naftifine hydrochloride, bucinnazine hydrochloride, flunarizine hydrochloride, and cinnarizine (Fig. 1). During the last ten years, there were significant reports on hydroboration of alkynes through homogeneous transition metal catalysts that usually require phosphine and nitrogen based ligands with high catalyst loading to produce good yield and high selectivity, which limits its commercial application in the industry.[10]

In the case of heterogeneous catalysts, Cu-nanocellulose sponge, Cu–$CuFe_2O_4$, copper nanospheres, Cu nanocubes, polyhedral Cu_2O, Cu powder, $CuFe_2O_4$, nano-Cu@Si, Fe_3O_4

[a]*Department of Biological Sciences, Pusan National University, Busan 46241, Korea. E-mail: bhyoun72@pusan.ac.kr*

[b]*Department of Chemistry, Madanapalle Institute of Technology & Science, Madanapalle, Chittoor 517 325, Andhra Pradesh, India*

[c]*Department of Chemistry and Chemistry Institute for Functional Materials, Pusan National University, Busan 46241, Korea. E-mail: chemistry@pusan.ac.kr*

[d]*Clean Fuel Research Laboratory, Korea Institute of Energy Research, Daejeon 34129, Korea. E-mail: jcpark@kier.re.kr*

[e]*Department of Chemistry, Korea University, 145 Anam-ro Seongbuk-gu, Seoul 02841, Korea*

† Electronic supplementary information (ESI) available. See https://doi.org/10.1039/d2ra04668g

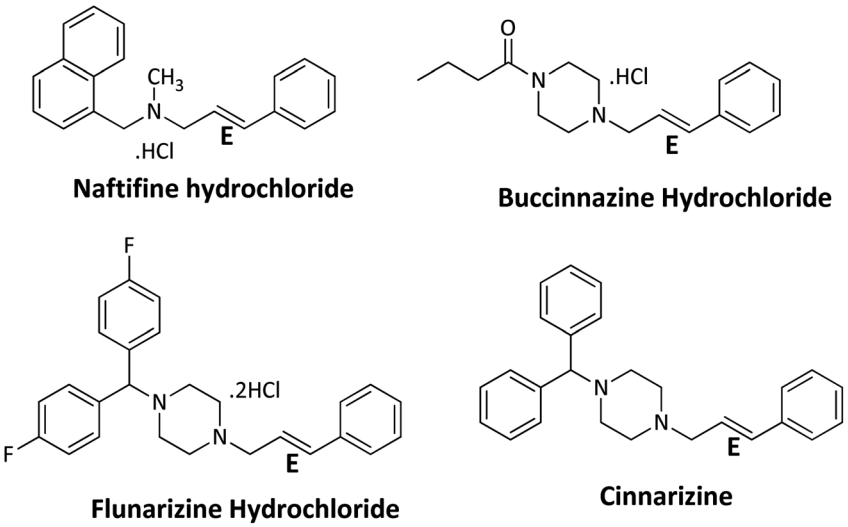

Fig. 1 Important drugs represent *E*-structure.

have been widely used to effect hydroboration of alkynes.[11] However, there are some drawbacks associated with the preparation of those catalysts are need for stoichiometric equivalents of reducing agents, high boiling solvents, additives, surfactants, and ligands. In addition, some catalysts are highly active only in the presence of phosphine ligands or excess base or elevated temperature, or intolerant to internal alkynes. Hence, developing a new methodology to prepare highly active and long-lived supported CuO nanocatalysts without any promoter has important significance for the activation and conversion of alkynes.

In the present work, a high-performance and long-lived CuO/CNF nanocatalyst in one pot has been prepared by a simple solid-state grinding followed by thermal treatment under nitrogen flow without the use of solvent, surfactants, and harmful reducing reagents. Hydroboration of alkyne was chosen as a probe reaction to evaluate the CuO/CNF nanocatalyst.

2. Experimental section

2.1 Chemicals

Copper(II) nitrate trihydrate ($Cu(NO_3)_2 \cdot 3H_2O$, Daejung, 99%) and carbon nanofibers (>98%, $D \times L$ 100 nm × 20–200 μm, Aldrich) were used as received without further purification. Phenylacetylene (99%) and other starting materials were procured from Aldrich and TCI Korea. All chemicals were used without further purification. The crude products were analyzed using a gas chromatography-mass spectrometry (GC-MS) system (QP2010SE, Shimadzu Corp.). All purified products after column chromatography were characterized by ^{1}H NMR (Agilent NMR, 400 MHz).

2.2 Synthesis of the CuO/CNF nanocatalyst

For the synthesis of the CuO/CNF catalyst, 1.2 mmol of $Cu(NO_3)_2 \cdot 3H_2O$ (0.285 g) and 25 mmol of carbon nanofibers (0.30 g) were homogeneously mixed with SamplePrep methacrylate grinding balls (diameter: 3/4 inch) using a high-energy ball mill (SPEX 8000M Mixer/Mill®) with 1725 rpm. After mixing for 5 min, the mixed powder sample was transferred to a stainless steel reactor (18 mm outer diameter, 1.0 mm wall thickness, 115 mm height). The mixture was then heated to 90 °C at a ramping rate of 9 °C min^{-1} under a closed reaction system, followed by aging at the same temperature for 1 h. Next, the mixed powder was cooled to room temperature. After that, the reactor was reheated to 220 °C at the ramping rate of 5.5 °C min^{-1} up to 220 °C under a flow of N_2 (100 mL min^{-1}); then it was thermally treated at the same temperature for 2 h. Finally, the resulting black powder was cooled to room temperature and then recovered.

2.3 Characterization

Scanning electron microscopy (SEM) was performed on a NovaNano SEM 450/FEI. For SEM analysis, a few drops of the colloidal solutions were placed on the small pieces (5 mm × 5 mm) of a silicon wafer, followed by drying in air. Transmission electron microscopy (TEM) images were obtained using a F200/JEOL operated at 200 kV. The TEM samples were prepared by placing a few drops of the colloidal solutions on nickel grids coated with formvar carbon film (Ted Pella, Inc.). The X-ray diffraction (XRD) patterns of the nanocatalyst were used to identify peak shape and crystallinity on a high-power (9 kW) powder X-ray diffractometer. A Rigaku D/MAX-2500 X-ray diffractometer with Cu Kα radiation was used for phase analysis. All diffraction patterns were collected at 2θ values between 20° and 80° using a step size of 3° min^{-1}. The crystallite sizes were estimated from the XRD using Scherrer equation: $L = K\lambda/\beta \cos\theta$, where L is the average particle (crystallite) size, K is the Scherrer constant related to the shape and index (hkl) of the crystals, λ is the wavelength (0.15406 nm) of the X-rays, β is the value of full width at half maximum (FWHM) of the peak in radians, and θ is the Bragg angle. The N_2 sorption isotherms were measured at −196 °C with a TriStar II 3020 surface area analyzer. Before measurement, the samples were degassed in a vacuum at 150 °C for 4 h.

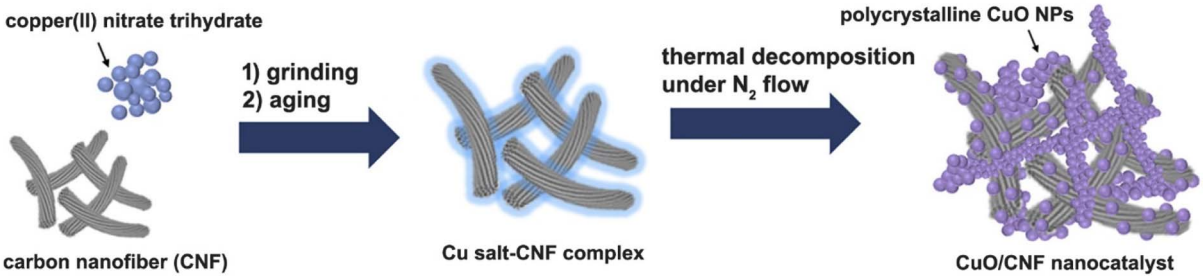

Scheme 1 A brief synthesis scheme of CuO/CNF nanocatalyst.

2.4 Experimental procedure for hydroboration reaction of phenylacetylene

In a typical synthesis procedure, to a 5 mL screw-capped vial, 4 mg of CuO/CNF catalyst (23.8 wt% CuO), phenylacetylene (100 mg, 0.9803 mmol), B_2Pin_2 (299 mg, 1.176 mmol), KO^{t}Bu (11 mg, 0.09803 mmol) and methanol (2 mL) were charged. The mixture was then purged with argon about 15 min and closed with cap. Then, the vial was kept in a 40 °C preheated oil bath

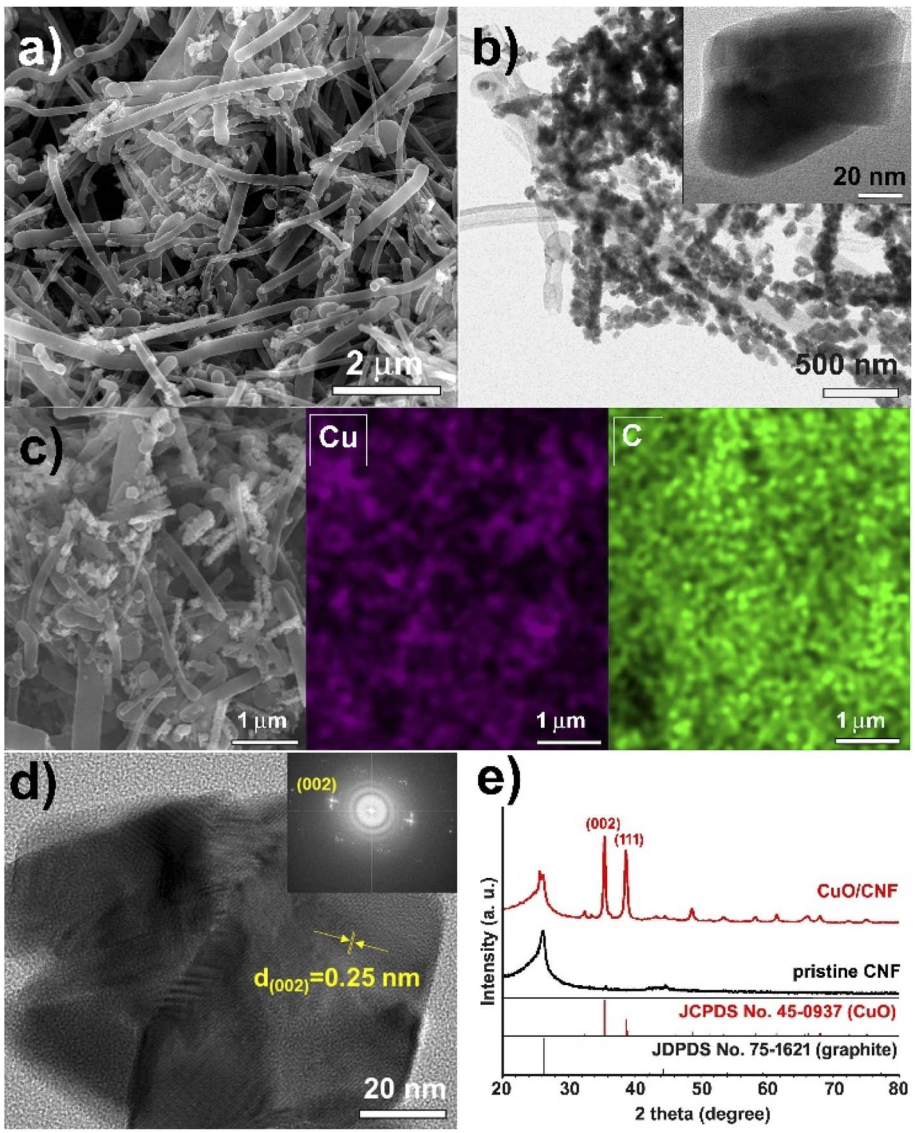

Fig. 2 (a) SEM image, (b) low-resolution TEM image, (c) elemental (Cu and C) mapping images, (d) HRTEM image, and (e) XRD pattern of CuO/CNF nanocatalyst.

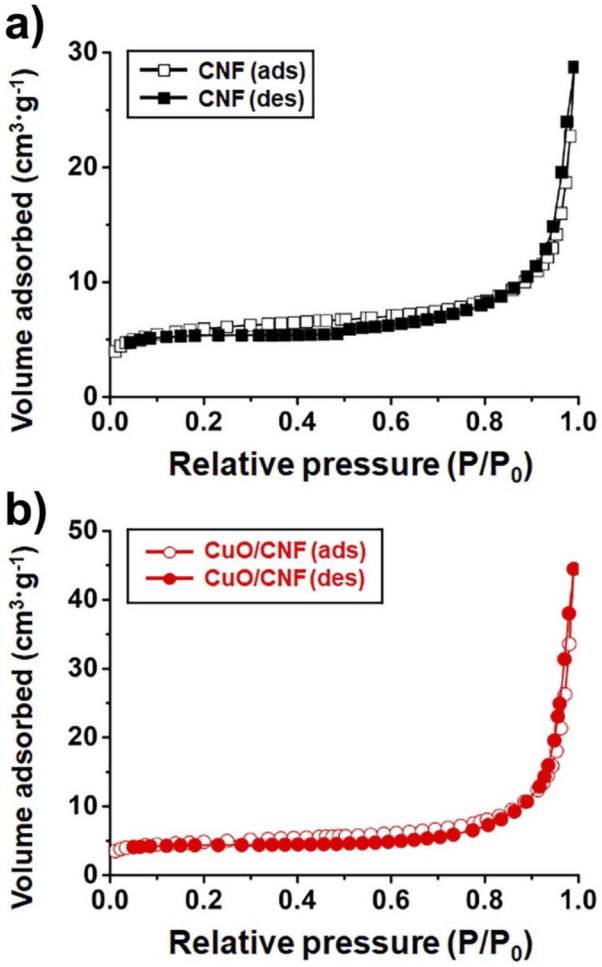

Fig. 3 N_2 adsorption/desorption isotherms of (a) pristine CNF and (b) CuO/CNF nanocatalyst.

for 12 h under magnetic stirring. After the maintenance, the vial was cooled to RT, passed through a celite bed followed by extraction with diethyl ether and washed with water and the solvent was evaporated through a rotary evaporator. The crude product was subjected to analyze by GC-MS. The residue was purified by column chromatography using ethyl acetate and hexane.

3. Results and discussion

3.1 Synthesis of the CuO/CNF catalyst

The CuO nanoparticles supported on the surfaces of CNF were obtained using a simple grinding and aging method of the hydrated copper salt, followed by its thermal treatment under N_2 (Scheme 1). To prepare a 23.8 wt% CuO-loaded catalyst, the $g_{Cu\ salt}/g_{CNF}$ ratio of 0.95 was used. First, $Cu(NO_3)_2 \cdot 3H_2O$ crystals, which have a melting point of 114 °C could be adsorbed on the carbon surfaces of CNFs by grinding them at room temperature and subsequently aging at 90 °C for 1 h in a tumbling oven. After the aging step to widely contact the Cu salt on the carbon supports, the polycrystalline CuO nanoparticles were generated by thermal treatment at 220 °C under a flow of N_2. The scanning electron microscopy (SEM) and transmission electron microscopy (TEM) images show incorporated CuO nanoparticles with *ca.* 90 nm (Fig. 2a and b). The single CuO particle anchored on the carbon support can clearly be observed (inset of Fig. 2b). The SEM elemental mapping of copper (violet) and carbon (green) demonstrated uniform particle dispersion (Fig. 2c). The high-resolution TEM (HRTEM) image exhibits a polycrystalline structure in which single-crystalline domains are observed to be *ca.* 30 nm (Fig. 2d). The high-resolution TEM(HRTEM) image and the corresponding Fourier-transform (FT) patterns indicated the formation of

Table 1 Optimization of CuO/CNF for the synthesis of alkenyl boronates using phenylacetylene and bis(pinacolato)diboron[a]

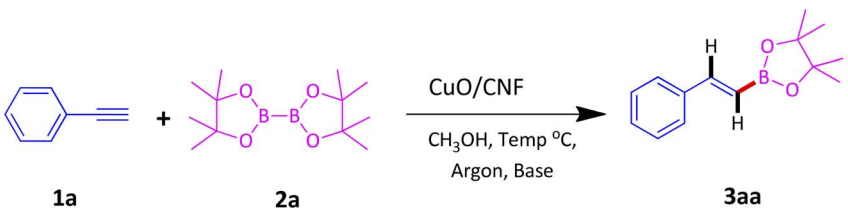

1a 2a 3aa

Entry	Catalyst (mg)	Base	Temp. (°C)	Conv.[b] (%) **3aa**
1	CuO/CNF (2)	—	25	59
2	CuO/CNF (2)	—	40	74
3	CuO/CNF (2)	K_2CO_3	40	82
4	CuO/CNF (2)	KO^{t}Bu	25	87
5	CuO/CNF (2)	KO^{t}Bu	40	98 (93)[c]
6	CuO/CNF (2)	KO^{t}Bu	40	69[d]
7	Recovered from #5	KO^{t}Bu	40	96
8	Recovered from #7	KO^{t}Bu	40	94
9	Recovered from #8	KO^{t}Bu	40	91
10	Recovered from #9	KO^{t}Bu	40	89

[a] Experimental conditions: phenylacetylene (0.49 mmol), B_2Pin_2 (0.588 mmol), CuO/CNF (2 mg), base (10 mol%), methanol (1 mL) under argon, 40 °C, 12 h. [b] Conversion determined by GC-MS. [c] Isolated yield. [d] 0.98 mmol of phenylacetylene were used.

Table 2 Substrate tolerance of various alkynes over CuO/CNF nanocatalyst[a]

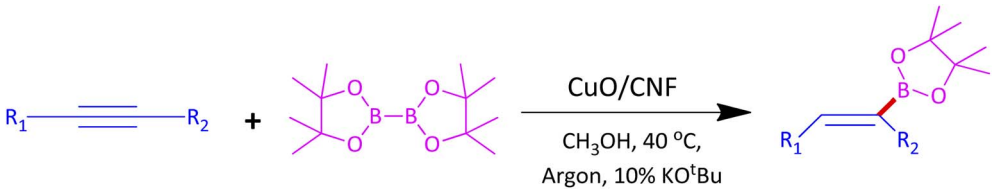

Entry	Alkyne	Product	Conv.[b] (%)
1	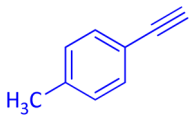	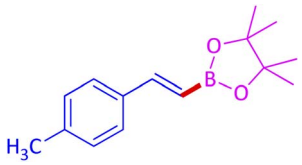	96 (93)[c]
2	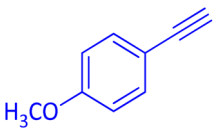	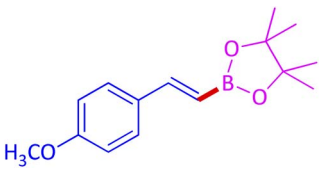	93 (89)[c]
3	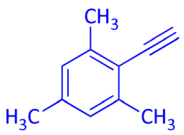	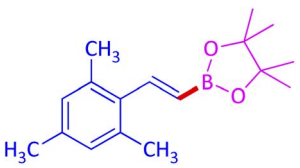	85 (79)[c]
4	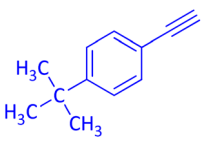	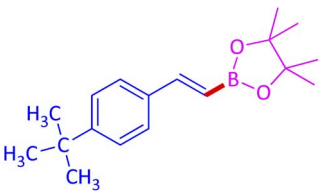	88 (82)[c]
5	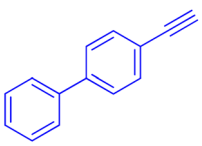	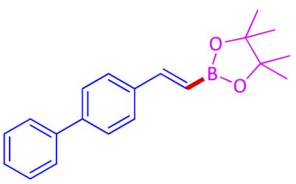	91 (85)[c]
6	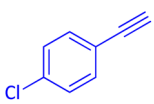	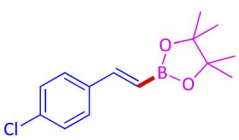	86 (81)[c]
7	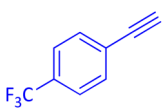	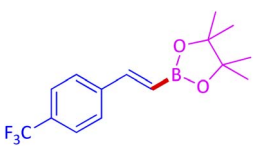	85 (83)[c]
8	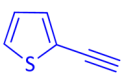	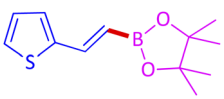	91 (87)[c]

Table 2 (*Contd.*)

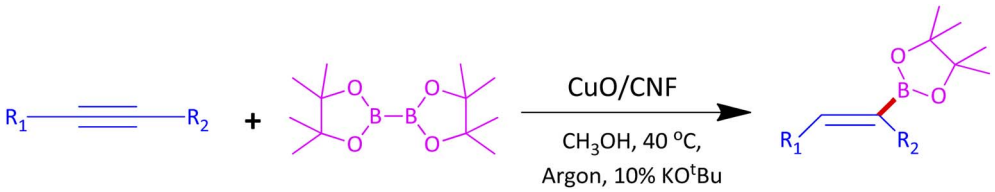

Entry	Alkyne	Product	Conv.[b] (%)
9	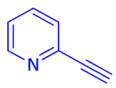	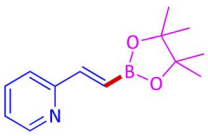	89 (84)[c]
10	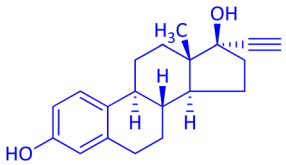	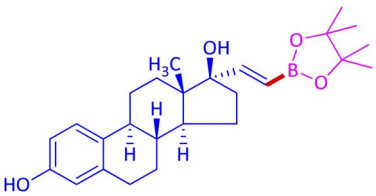	74
11	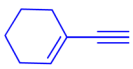	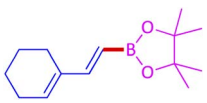	97
12	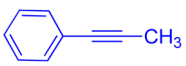	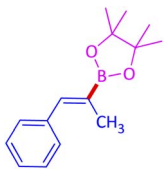	86 (81)[c]

[a] Experimental conditions: alkyne (1 mmol), B_2Pin_2 (1.2 mmol), CuO/CNF (2 mg), base (10 mol%), methanol (1 mL) under argon, 40 °C, 12 h. [b] Conversion determined by GC-MS. [c] Isolated yield.

copper(II) oxide crystals with a distance of 0.25 nm between neighboring fringes, matching well with the (002) planes of monoclinic CuO (Fig. 2d). In the X-ray diffraction (XRD) pattern of pristine CNF, graphite peaks were mainly observed at $2\theta = 26.2°$ and 44.4°; corresponding to the reflections of the (002) and (101) planes of graphitic carbon (JCPDS No. 75-1621) (Fig. 2e). The XRD pattern of the CuO/CNF nanocatalyst shows that CuO nanoparticles are well-matched with the monoclinic CuO phases (JCPDS No. 45-0937; space group, *C*2/*c*). The single-crystalline domains of CuO particle estimated from the FWHM of the (002) diffraction peak at $2\theta = 35.5°$ was 28 nm.

The N_2 sorption experiments for pristine CNF and CuO/CNF nanocatalyst exhibited type II adsorption–desorption hysteresis (Fig. 3a and b). The nitrogen isotherms indicate their macroporous or nonporous characteristic. The BET surface areas of the pristine CNF and CuO/CNF were very low, calculated to be 21.9 $m^2\ g^{-1}$ and 17.8 $m^2\ g^{-1}$. The very small pore volumes both in the pristine CNF were observed as 0.044 $cm^3\ g^{-1}$, and 0.069 $cm^3\ g^{-1}$ in the CuO/CNF nanocatalyst (Fig. 3).

We began our investigation with highly dispersed CuO/CNF NPs as a catalyst for the hydroboration of phenylacetylene for screening optimal reaction conditions, and Table 1 summarizes the results. Initially, we chose methanol as the solvent and 25 °C as the reaction temperature under argon atmosphere (to avoid glaser homocoupling of alkynes) for optimizing the catalyst. At 25 °C without base afforded only 59% conversion for 12 h stirring whereas increasing temperature to 40 °C led to 74% (entry 1 and 2, Table 1). Upon including 10 mol% K_2CO_3 as a base at 40 °C, the conversion of **3aa** was improved to 82% (entry 3, Table 1). But when base changed to KO^{t}Bu, conversion was good to excellent at 25° and 40 °C along with outstanding *E*-regioselectivity (Entries 4 and 5, Table 1). The conversion was reduced to 69% when phenylacetylene moles were increased to 0.98 mmol which seems 2 mg of catalyst is minimum requirement for optimum conversion (entry 6, Table 1). The catalyst recovered from entry 5 upon centrifugation and drying followed by stored under argon after each run have been reused four times successfully with good conversions (entries 7 to 10, Table 1).

The protocol with a CuO/CNF catalyst was applicable to various alkynes bearing both electron donating and electron withdrawing functionalities (Table 2). Terminal alkynes with

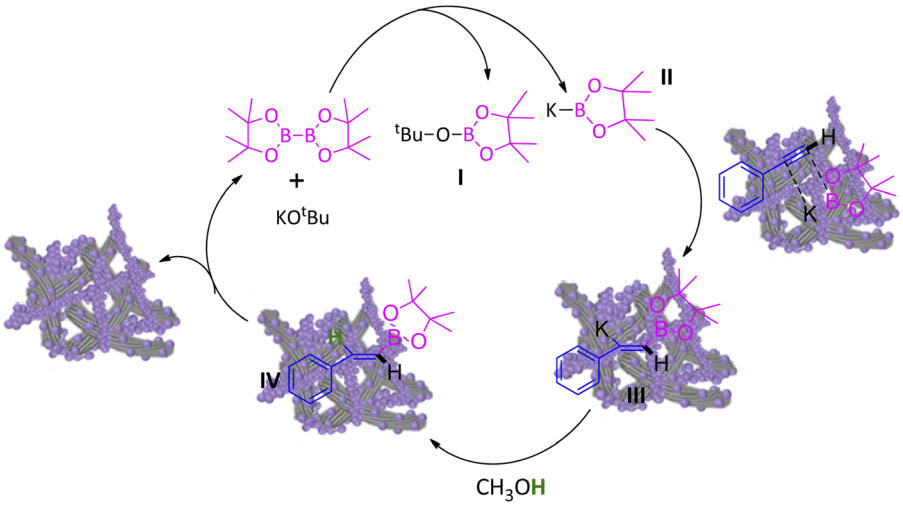

Scheme 2 Proposed mechanism for hydroboration of alkynes on the surface of CuO/CNF.

methyl, methoxy, chloro, *t*-butyl, trifluoromethyl and phenyl at para positions were well tolerated to afford corresponding *E*-alkenyl boronates in excellent yields (Entries 1–6, Table 2). Sterically hindered 2-ethynylmesitylene was also compatible with our CuO/CNF catalyst (entry 7, Table 2). Heterocyclic derivatives such as 2-ethynyl thiophene and 2-ethynyl pyridine were also borylated efficiently (Entries 8 & 9, Table 2). A synthetic hormone 17α-ethynylestradiol was also produced corresponding *E*-alkenyl boronate in moderate yield (entry 10, Table 2).[12] More importantly, CuO/CNF was highly chemoselective to alkyne as no reaction on the olefin was noticed when 1-ethynylcyclohexene was subjected to hydroboration reaction (entry 11, Table 2). Particularly, this protocol also works for the internal alkyne such as 1-phenyl-1-propyne was also afforded corresponding alkenyl boronate in high yield (entry 12, Table 2). From the above results, CuO/CNF was highly tolerant to a broad range of functional groups, whatever the substitution pattern, and the hydroborylated products were isolated in good to excellent yields and showed outstanding *E*-regioselectivity. The crude products (entry 10 and 11, Table 2) without column chromatography isolation were subjected to ^{1}H NMR analysis (see ESI†) and showed doublets at 5.67 ppm with the *J* value of 18.4 Hz (entry 10) and 5.42 ppm with the *J* value of 18.2 Hz (entry 11) that corresponds to exclusive formation of *E*-regioisomer.

3.2 Catalytic cycle

A plausible mechanism for hydroboration of alkynes has been proposed in Scheme 2.[11f] Initially, the reaction of KO^{t}Bu with B_2Pin_2 led **I** and **II**. Adsorption of phenyacetylene and **II** on the surface of CuO/CNF provides intermediate **III**, followed by replacement of potassium of **III** by protonation with the assistance of solvent CH_3OH regenerates final product **IV** and the CuO/CNF catalyst.

4. Conclusions

In this paper we have reported that copper(II) oxide nanoparticles supported on carbon nanofiber were prepared in one-pot utilizing a simple solid-state grinding followed by thermal treatment under nitrogen flow in the absence of surfactant, reducing agent and solvent. The catalyst was used for the preparation of vinylboronates under heterogeneous conditions. This technique eliminates the use of any ligand or additive, and is applied to a wide range of terminal, and internal alkynes including steroid derivative affording good to excellent yields with high regioselectivites under mild conditions. The catalyst also possesses good recyclability and excellent chemoselectivity.

Conflicts of interest

There are no conflicts to declare.

Acknowledgements

This work was supported by a 2 Year Research Grant of Pusan National University.

References

1 (*a*) M. J. Ndolomingo, N. Bingwa and R. Meijboom, *J. Mater. Sci.*, 2020, **55**, 6195–6241; (*b*) P. K. Baroliya, J. Chopra, T. Pal, S. Maiti, S. A. Al-Thabaiti, M. Mokhtar and D. Maiti, *ChemCatChem*, 2021, **13**, 4655–4678; (*c*) M. Sankar, Q. He, R. V. Engel, M. A. Sainna, A. J. Logsdail, A. Roldan, D. J. Willock, N. Agarwal, C. J. Kiely and G. J. Hutchings, *Chem. Rev.*, 2020, **120**, 3890–3938.

2 (*a*) C. Wen, Y. Cui, W.-L. Dai, S. Xie and K. Fan, *Chem. Commun.*, 2013, **49**, 5195–5197; (*b*) Z. Huang, F. Cui, H. Kang, J. Chen, X. Zhang and C. Xia, *Chem. Mater.*, 2008, **20**, 5090–5099; (*c*) Z. Li, T. He, L. Liu, W. Chen, M. Zhang, G. Wu and P. Chen, *Chem. Sci.*, 2017, **8**, 781–788; (*d*) M. B. Gawande, A. Goswami, F.-X. Felpin, T. Asefa, X. Huang, R. Silva, X. Zou, R. Zboril and R. S. Varma, *Chem. Rev.*, 2016, **116**, 3722–3811.

3 (*a*) X. Cui, X. Dai, Y. Deng and F. Shi, *Chem. - Eur. J.*, 2013, **19**, 3665–3675; (*b*) A. B. Laursen, I. C. Man, O. L. Trinhammer,

J. Rossmeisl and S. Dahl, *J. Chem. Educ.*, 2011, **88**, 1711–1715; (*c*) D. Formenti, F. Ferretti, F. K. Scharngal and M. Beller, *Chem. Rev.*, 2019, **119**, 2611–2680.

4 (*a*) J. Cho, L. Xu, C. Jo and R. Ryoo, *Chem. Commun.*, 2017, **53**, 3810–3813; (*b*) S. H. Joo, S. J. Choi, I. Oh, J. Kwak, Z. Liu, O. Terasaki and R. Ryoo, *Nature*, 2001, **412**, 169–172; (*c*) N. Narayan, A. Meiyazhagan and R. Vajtai, *Materials*, 2019, **12**, 3602–3616.

5 (*a*) W. Luo, U. Deka, A. M. Beale, E. R. H. van Eck, P. C. A. Bruijnincx and B. M. Weckhuysen, *J. Catal.*, 2013, **301**, 175–186; (*b*) A. Lekhal, B. J. Glasser and J. G. Khinast, *Chem. Eng. Sci.*, 2004, **59**, 1063–1077; (*c*) J. A. Bergwerff, T. Visser, G. Leliveld, B. D. Rossenaar, K. P. de Jong and B. M. Weckhuysen, *J. Am. Chem. Soc.*, 2004, **126**, 14548–14556.

6 (*a*) M. K. van der Lee, J. van Dillen, J. H. Bitter and K. P. de Jong, *J. Am. Chem. Soc.*, 2005, **127**, 13573–13582; (*b*) M. Che, Z. X. Cheng and C. Louis, *J. Am. Chem. Soc.*, 1995, **117**, 2008–2018; (*c*) P. Burattin, M. Che and C. Louis, *J. Phys. Chem. B*, 1999, **103**, 6171–6178.

7 (*a*) L. Jiao and J. R. Regalbuto, *J. Catal.*, 2008, **260**, 329–341; (*b*) M. Schreier and J. R. Regalbuto, *J. Catal.*, 2004, **225**, 190–202; (*c*) M. Hartmann, A. Pöppl and L. Kevan, *J. Phys. Chem.*, 1996, **100**, 9906–9910.

8 (*a*) B. Mile, D. Stirling, M. A. Zammitt, A. Lovell and M. Webb, *J. Catal.*, 1988, **114**, 217–229; (*b*) J. Panpranot, J. G. Goodwin and A. Sayari, *Catal. Today*, 2002, **77**, 269–284; (*c*) J.-S. Girardon, A. S. Lermontov, L. Gengembre, P. A. Chernavskii, A. Griboval-Constant and A. Y. Khodakov, *J. Catal.*, 2005, **230**, 339–352.

9 T. M. Eggenhuisen, J. P. d. Breejen, D. Verdoes, P. E. d. Jongh and K. P. d. Jong, *J. Am. Chem. Soc.*, 2010, **132**, 18318–18325.

10 (*a*) J. Liu, C. Wu, T. Hu, W. Yang, Y. Xie, Y. Shi, Q. Liu, Y. Shao and F. Zhang, *J. Org. Chem.*, 2022, **87**, 3442–3452; (*b*) C. E. Tucker, J. Davidson and P. Knochel, *J. Org. Chem.*, 1992, **57**, 3482–3485; (*c*) D. P. Ojha and K. R. Prabhu, *Org. Lett.*, 2016, **18**, 432–435; (*d*) G. Zhang, H. Zeng, S. Zheng, M. C. Neary and P. A. Dub, *ACS Catal.*, 2022, **12**, 5425–5429; (*e*) H. Yoshida, I. Kageyuki and K. Takaki, *Org. Lett.*, 2014, **16**, 3512–3515; (*f*) N. Gorgas, B. Stöger, L. F. Veiros and K. Kirchner, *ACS Catal.*, 2018, **8**, 7973–7982; (*g*) R. J. Procter, M. Uzelac, J. Cid, P. J. Rushworth and M. J. Ingleson, *ACS Catal.*, 2019, **9**, 5760–5771; (*h*) R. Mamidala, V. K. Pandey and A. Rit, *Chem. Commun.*, 2019, **55**, 989–992; (*i*) M. Zhong, Y. Gagné, T. O. Hope, X. Pannecoucke, M. Frenette, P. Jubault and T. Poisson, *Angew. Chem., Int. Ed.*, 2021, **60**, 14498–14503; (*j*) K. Jaiswal, K. Groutchik, D. Bawari and R. Dobrovetsky, *ChemCatChem*, 2022, **14**, e202200004.

11 (*a*) C. Zhang, M. Zhou, S. Liu, B. Wang, Z. Mao, H. Xu, Y. Zhong, L. Zhang, B. Xu and X. Sui, *Carbohydr. Polym.*, 2018, **191**, 17–24; (*b*) X. Zeng, C. Gong, H. Guo, H. Xu, J. Zhang and J. Xie, *New J. Chem.*, 2018, **42**, 17346–17350; (*c*) B. Wang, L. Gao, H. Yang and G. Zheng, *ACS Appl. Mater. Interfaces*, 2021, **13**, 47530–47540; (*d*) H.-Y. Tsai, M. Madasu and M. H. Huang, *Chem. - Eur. J.*, 2019, **25**, 1300–1303; (*e*) S. Thoka, M. Madasu, C.-F. Hsia, S.-Y. Liu and M. H. Huang, *Chem.–Asian J.*, 2017, **12**, 2318–2322; (*f*) J. Zhao, Z. Niu, H. Fu and Y. Li, *Chem. Commun.*, 2014, **50**, 2058–2060; (*g*) B. Mohan and K. H. Park, *Appl. Catal., A*, 2016, **519**, 78–84; (*h*) V. S. Rawat and B. Sreedhar, *Synlett*, 2014, **25**, 1132–1136.

12 A. Z. Aris, A. S. Shamsuddin and S. M. Praveena, *Environ. Int.*, 2014, **69**, 104–119.